Catalysis Today 430 (2024) 114520

Contents lists available at ScienceDirect

Catalysis Today

journal homepage: www.elsevier.com/locate/cattod

Modeling TiO_2/UV–vis bacterial inactivation: Useful tools for reactor optimization and design

R. Moreno [a], Samuel Moles [a,b,*], Maria P. Ormad [a,b], R. Mosteo [a,b], A. Monzón [a,c]

[a] Departamento de Ingeniería Química y Tecnologías del Medio Ambiente. Universidad de Zaragoza, Spain
[b] Instituto de Investigación en Ciencias Ambientales de Aragón (IUCA). Universidad de Zaragoza, Spain
[c] Instituto de Nanociencia y Materiales de Aragón (INMA). CSIS-Universidad de Zaragoza, Spain

ARTICLE INFO

Keywords:
Photorreactor
Kinetics
Inactivation
Photocatalysis
Modeling
Optimization

ABSTRACT

Heterogeneous photocatalysis applying TiO_2 based catalysts has been widely studied for removing inorganic and organic compounds from water and for bacterial inactivation. This available and low-cost catalyst has demonstrated to be effective in the removal of organic pollutants and inactivation of pathogenic bacteria from water. The design of proper types of industrial-scale photoreactors has not been yet successfully implemented, probably due to the conceptual complexity of modeling this process in real wastewater. As a result, TiO_2 based photocatalysis is still considered an effective but energetic-inefficient process. In this work, *Escherichia coli* (gram-positive) and *Enterococcus sp* (gram-negative) were selected for studying the kinetics of TiO_2 photocatalysis. Since several approaches, such as fist-order kinetics, are not truly representative of the bacterial inactivation process, the experimental data were fitted to different mathematical models, such as Gompertz model, which has demonstrated to describe the process properly. Moreover, the effect of the main variables of the process in the inactivation kinetic constant of the Gompertz model has ben studied. More precisely, light intensity, water matrix, catalyst concentration and bacteria have been under study and their effect has been included in the kinetic equation. Finally, operational and construction parameters of a 20 m^3/d annular photoreactor for bacterial inactivation has been successfully optimized applying the proposed kinetic model.

1. Introduction

The presence of pathogenic microorganisms in waters is an issue of special concern due to the potential risk of waterborne diseases. Moreover, the presence of pharmaceuticals in waters, such as antibiotics, promotes the presence of Antimicrobial Resistant Microorganisms. According the World Health Organization (WHO) the dead associated to Antimicrobial Resistance (AMR) in 2050 are stimated in 10 million presenting an important hazard for the human health worldwide [1,2]. Bacteria, viruses and protozoa can be naturally present in waters or introduced as a result of the human activity [3]. Since the detection of some of these pathogens is not easy, a group of indicator microorganisms has been chosen to determine water quality [4]. Coliform bacteria are common indicators, such as *Escherichia coli* owing to its presence in human intestinal flora [5]. These bacteria present a greater persistence in comparison to some other pathogens [5]. Moreover, *Enterococcus sp* is reported to be also useful indicators belonging to the gram-negative group. Consequently, coliform bacteria inactivation has been widely studied through several processes [6–8].

Generally, lacking a legal requirement, Wastewater Treatment Plants (WWTPs) are not designed to reduce significantly the microbiological load of the effluents. As a result, these agents are incorporated into natural waters. The conventional and the most extensively treatment used in water disinfection has been chlorination [9]. However, the literature points to the generation of carcinogens by-products (e.g. trihalomethanes) due to the reaction of organic matter and chlorine [9], consequently they are controlled in the current EU Drinking Water Directive 2023. As a result, previous treatments should be applied to remove or significantly reduce organic matter present in treated urban effluent, before applying chlorination.". Nowadays, cleaner disinfection treatments such as Advanced Oxidation Processes (AOPs) are under study to substitute conventional treatments. The common denominator of these processes is the generation of highly Reactive Oxygen Species (ROS), such as hydroxyl radicals, which are able to eliminate microorganisms and other recalcitrant pollutants [10,11]. For instance, UV-based photocatalysis, ultrasound, ozonation, photo-Fenton have

* Corresponding author at: Departamento de Ingeniería Química y Tecnologías del Medio Ambiente. Universidad de Zaragoza, Spain.
E-mail address: sma@unizar.es (S. Moles).

https://doi.org/10.1016/j.cattod.2024.114520
Received 2 November 2023; Received in revised form 21 December 2023; Accepted 10 January 2024
Available online 12 January 2024

been applied for disinfection and/or oxidation of inorganic and organic pollutants in order to reuse treated urban wastewater [12,13].

Photocatalysis could be a feasible substitution for conventional disinfection processes. However, it is necessary to minimize the cost of the treatment. Photocatalysis has proved its efficiency in microbial disinfection, especially using titanium dioxide (TiO_2) as semiconductor catalyst, since it is relatively abundant, cheap and environmentally-friendly [14–16]. The photocatalysis mechanism starts with the electron excitation with energy in the range 300–390 nm, which produces positive holes in the valence band (h^+_{vb}) and negative electrons in the conduction band (e^-_{cb}) [10,17]. Afterwards, these holes and electrons can respectively react with water or oxygen molecules adsorbed to the surface of the catalyst and form reactive oxygen species (ROS) [17].

The main and the first microbial targets of these ROS are the extracellular ones (in bacteria, the cellular membrane and the peptidoglycan of the cellular wall). However, the peptidoglycan is a very porous polymer which could delay hydroxyl radicals and superoxide anions to permeate to the inner membrane [18]. Gram-positive bacteria (such as *Enterococcus sp.*) have a thicker peptidoglycan layer than Gram-negative bacteria (such as *E.coli.*), therefore this has been the explanation given by some researchers who have exposed species of the two groups to the same photocatalytic treatment and have seen that Gram-positive bacteria were more resistant than Gram-negative [7,19,20]. However, the role of the peptidoglycan in terms of microbial inactivation it is not well established yet, and consequently it is not appropriate to use the thickness of the peptidoglycan layer as the only justification for the differences in the inactivation rates between Gram-positive and Gram-negative bacteria.

Parameters such as H_2O_2 addition, sample pH and the amount of wavelength of the radiation employed, require specific research depending on the type of matrix and its uses after treatment [21,22]. Chick proposed the first kinetic model in 1908 [23], a first order inactivation kinetic to model linear inactivation curves. However, this model not always describe observed deviations in the processes of bacterial inactivation, since this inactivation presents some non-lineal patterns shapes, such as shoulders (initial lag in which bacteria are eliminated more slowly) or tails (final lag in bacteria inactivation). The fitting of experimental bacterial inactivation data to properly selected kinetic models can provide useful information for reactor design purposes [24–28].

According to the literature, photocatalysis is not considered an energy efficient process due to the high power consumption [12]. Nowadays the implementation of photocatalysis is still under study at a Technology Readiness Level (TRL) 5 [29]. To improve photo-reactors design it is necessary to stablish feasible microbial inactivation kinetics and study the influence of the main operational variables such as light intensity or TiO_2 concentration in real wastewater [30,31]. Photo-reactor modeling is more difficult in comparison to other conventional reactors, since, in addition to momentum, heat and mass transfer, radiation transfer rates must be also considered. The attenuation of light intensity by the absorption and scattering effects of suspended TiO_2 particles, implies solving the radiative transfer equation (RTE) to calculate the local volumetric rate of photon absorption (LVRPA) in the reactor [27,28,32–35]. In this regard, Cassano et al. have developed rigorous, but quite complex, models which are difficult to apply for reactor engineering purposes [33,36]. Some researchers have pointed that light distribution in the photo-reactor could be modeled by Lambert-Beer's law using an apparent extinction coefficient in which both absorption and scattering effects are included [37–39] for chemical reactions or elimination of pollutants in water. However, this law has some limitations in heterogeneous systems which should be taken into account. First, Lambert-Beer's law assumes a homogenous medium, an assumption that may not hold in complex matrix as wastewater, with non-uniform catalyst distribution and diverse phases, such as solids in suspension [40,41]. Additionally, it should be remarked that Lambert-Beer's law is designed for single-component systems and, as a result may not accurately model the interactions in multicomponent systems [28]". In any case, Lambert-Beer's law is enough valid for the applicability of the developed model here.

Table 1
Physicochemical and microbiological parameters of the four water samples.

Parameter	Sample 1	Sample 2	Sample 3	Sample 4
pH	7.4	7.7	8.4	7.3
Conductivity (μS/cm)	1400	1100	1063	1500
Turbidity (NTU)	22	18	15	45
TSS (mg/l)	43	24	16	65
TOC (mg C/l)	24	27	38	15
COD (mg O_2/l)	65	40	50	-
E.coli log (UFC/100 ml)	6.6	5.5	4.8	3.8
*Enterococcus sp.*log(UFC/100 ml)	4.7	4.6	2.9	3.1

Few studies in literature assess the influence of operational conditions in real wastewater of this process for gram-positive and gram negative bacteria. Consequently, it is necessary to develop a suitable kinetic model of the TiO_2 photocatalytic inactivation of both, gram-positive and gram-negative bacteria, which can be applied in real wastewater. Therefore, in this research work, the goal is to develop a phenomenological model that describes bacterial inactivation kinetics, including the effect of the main operational variables in the kinetic constant (such as light intensity or catalyst concentration). Furthermore, we aim to propose an analytical model to design a pilot-scale annular photocatalytic reactor for wastewater disinfection based on the intrinsic kinetic and its geometry.

2. Materials and methods

Four sets of experiments were carried out to study bacterial inactivation, in each of which a different variable was studied: (i) type of coliform bacteria (gram-positive or gram negative); (ii) water matrix; (iii) TiO_2 concentration, and (iv) light intensity.

2.1. Samples

The experimental sets carried out in a saline solution (NaCl 0,9%) were made from in ultrapure water sterilized in autoclave at 121^0 C, presenting a pH of 6,4 and average values of turbidity (NTU); total suspended solids (TSS, mg/l), total organic carbon (TOC mg O_2/l), and chemical oxygen demand (COD, mg O_2/l) inferior than 1. Afterwards, the sterile saline solutions were fortified with the corresponding bacteria: *E.coli, Enterococcus sp.,* previously isolated from effluents from a municipal wastewater treatment plant (WWTP) in Spain, getting a bacterial suspension of 10^7-10^8 CFU/100 ml.

By contrast, for the experimental sets carried out in real wastewater, samples were collected at a real municipal wastewater treatment plant (WWTP) located in Navarra (Spain). The specific steps of this facility are screen, grit and grease separation, sedimentation and trickling filter. Physico-chemical and microbiological parameters of these water samples are shown in Table 1.

2.2. Bacterial analysis

Two methods were used to perform the bacterial analysis depending on the microbiological concentration. The standard method 9215 C was follow when the microbiological concentration was higher than $4{\cdot}10^3$ CFU/100 ml, making decimal dilutions if it is necessary. However, for microbiological concentrations lower than $4{\cdot}10^3$ CFU/100 ml, the analyses were conducted according to the membrane filtration methods UNE-EN ISO 9308–1 for *Escherichia coli* and UNEEN ISO 7899–2 for *Enterococcus sp*.

Concerning the culture, the samples were plated of MacConkey agar (Scharlau) for *E. coli*, and pink colonies were counted after 24-h

Table 2
Operational conditions analyzed in different experiments.

	Water sample	Treatment time (min)	[TiO_2] (g/l)	Light intensity (W/m^2)	Variable
Experimental set A	Saline solution	0-120	1	500	Time
Experimental set B	WWTP sample	120	1	500	Water composition
Experimental set C	Saline solution	10	0-2	500	TiO_2 concentration
Experimental set D	Saline solution	0-120	1	0-750	UVA dose

incubation at 42 °C. For *Enterococcus sp.*, the samples were plated on Slanetz and Bartley agar base (Scharlau), and dark red colonies were counted after 48-h incubation at 37 °C. The enumeration of the bacteria was expressed as CFU (colony-forming units) per 100 ml of sample (CFU/100 ml). The bacterial inactivation was expressed as $\log(N_t/N_0)$, where N_0 was the initial bacterial concentration and N_t the remaining bacterial concentration at time t.

2.3. Experimental setting

The experiments were divided in four sets (A-D) as shown in Table 2. As observed in the table, the values for light intensity and catalyst concentration in the experiments in which these are not considered as variables are 500 W/m^2 and 1 g/l respectively, which had been previously selected by other researchers [8,42].

For all experiments, a water volume of 100 ml was added in a 250 ml beaker and after adding the necessary amount of TiO_2 FN2, the beaker was placed in a solar chamber (SUNTEST CPS+/xls+). This system enabled reproduction of natural sunlight conditions in the laboratory. A quartz filter and an additional glass filter (Xenochrome 320) were used to cut off wavelengths below 320 nm, removing the UVB and UVC ranges. Therefore, the samples were exposed to wavelengths between 320 and 800 nm, corresponding to the UVA and visible bands. The solar chamber was equipped with a magnetic agitator and a regulator of intensity and time of exposure, as well as a temperature control. Maximum temperature reached in the solar chamber was 35 ºC, although the samples did not exceed 30 ºC.

2.4. Inactivation models

Kinetic equations used for the fitting of the experimental data were selected according to the inactivation curve shapes and by limiting the number of fitting parameters to two. The models selected were: Hom, Verhulst and modified Gompertz models.

Obtaining the values of the parameters of each model was carried out by fitting the experimental values to the corresponding equation by non linear regression using Microsoft Excel® Solver tool. As there are several orders of magnitude of difference between the experimental points, the relative root-mean-square-error (RRMSE) was chosen as the objective function to minimize and as the statistical parameter to assess the quality of the fitting. In the fitting of data from experimental set C, in which the variable was TiO_2 concentration, the conventional non-linear regression process was followed, by minimizing the root-mean-square-error (RRMSE) and by calculating the correlation coefficient (R^2), since there are not differences in several orders of magnitude between the experimental points.

(i) Hom model

Hom model is an empirical generalization of Chick model. Hom observed that the inactivation kinetics of algal-bacterial systems did not follow the traditional linear models, but they had curvilinear kinetics. The kinetic model proposed by Hom is given by:

$$N = N_0 \cdot \exp\left(-k_I \cdot t^m\right) \quad \leftrightarrow \quad r_I = -\frac{dN}{dt} = m \cdot {k_I}^{1/m} \cdot N \cdot \left(\ln\left(\frac{N}{N_0}\right)\right)^{(m-1)/m} \tag{1}$$

(ii) Inactivation Verhulst and Gompertz models:

Verhulst equation (usually known as logistic equation) and Gompertz equation were initially defined for microbial growth. However, they can be modified to predict bacterial inactivation by the introduction of a new parameter, the residual bacterial concentration (N_R) resulting in Eqs. (2) and (3), respectively, for Verhulst and Gompertz models:

$$r_I = -\frac{dN}{dt} = k_I \cdot N \cdot \left(N - N_R\right) \quad \leftrightarrow \quad N = \frac{N_R}{1 - \left(\frac{N_0 - N_R}{N_0}\right) \cdot \exp\left(-k_I \cdot N_R \cdot t\right)} = \frac{N_R}{1 - (1 - a_R) \cdot \exp(-k_I \cdot N_R \cdot t)} \quad ; \quad a_R = \frac{N_R}{N_0} \tag{2}$$

$$r_I = -\frac{dN}{dt} = k_I \cdot N \cdot \ln\left(\frac{N}{N_R}\right) \quad \leftrightarrow \quad N = N_0 \cdot \left(\frac{N_R}{N_0}\right)^{1-\exp(-k_I \cdot t)} = N_0 \cdot (a_R)^{1-\exp(-k_I \cdot t)} \quad ; \quad a_R = \frac{N_R}{N_0} \tag{3}$$

2.5. Photo-reactor modeling

The suggested model for an annular photo-reactor assumes (i) steady-state, (ii) negligible termal effects; (iii) unidirectional axial laminar flow; (iv) incompressible flow, as proposed by Cassano et al. in some studies [33,36]. Other researchers have reported that it is preferable turbulent flow operation in order to avoid catalyst deposition [10,37]. However, the values of bacterial inactivation constants calculated from the kinetic experiments are quite small (in water from WWTP, $4.45 \bullet 10^{-3} \pm 1.067\ min^{-1}$ average value for *E.coli* and $6.6910^{-3} \pm 4.187\ min^{-1}$ for *Enterococcus sp.*), and operating in turbulent regime would imply really high reactor lengths. Moreover, in the present work, it is shown that catalyst settling could be also avoided even operating in laminar flow. Therefore, one of the main requirements for the design and optimization of the photo-reactor has been that the Reynolds number (Re) was less than 2.100, in order to avoid the complex mathematical treatment linked to transient regime, but close to 2.100, so that TiO_2 aggregates do not settle and there is enough contact between the catalyst particles and bacteria. Some researchers also tried to model the behavior of an annular photo-reactor for bacterial disinfection operating

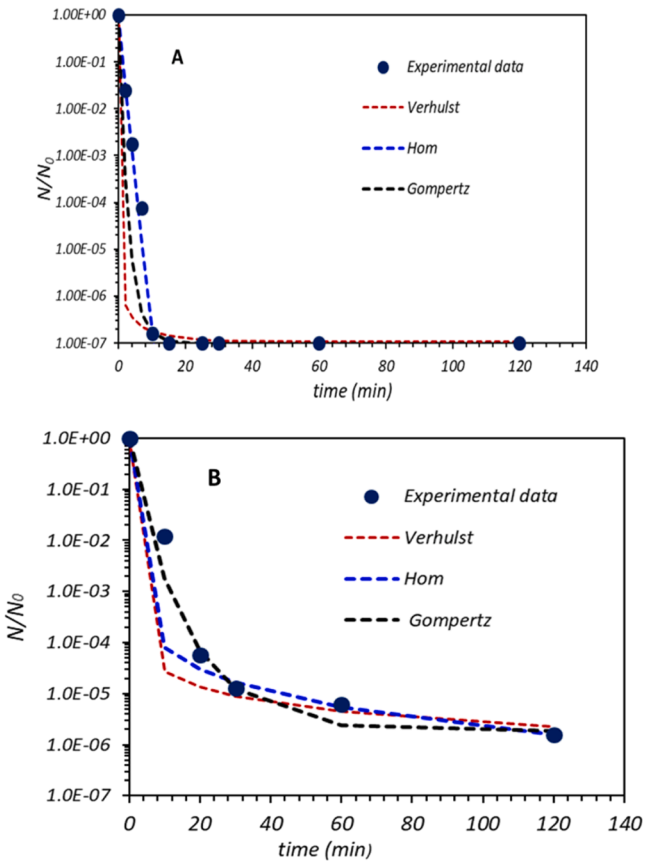

Fig. 1. Fitting of the results to mathematical models to the inactivation curves of *Escherichia coli* (A), *Enterococcus sp.* (B).

Table 3
Kinetic parameters of the mathematical models used for bacterial inactivation.

Model	Parameters	*E. coli*	*Enterococcus sp.*
Hom	k_I (min^{-m})	1.83	6.825
	m	0.928	0.140
	RRMSE	3.814	1.305
Verhulst	k_I (min^{-1})	$3.32 \bullet 10^{-2}$	$1.067 \bullet 10^{-4}$
	a_R	$9.10 \bullet 10^{-8}$	$3.46 \bullet 10^{-11}$
	RRMSE	3.033	1.929
Gompertz	k_I (min^{-1})	0.337	0.065
	a_R	$9.50 \bullet 10^{-8}$	$1.83 \bullet 10^{-6}$
	RRMSE	2.961	1.176

in laminar flow and suggested a similar model to the one presented in this work [43,44]. Bacterial diffusion in radial and axial coordinates has been neglected owing to bacterial high molecular weight, and consequently, their low diffusion coefficient in comparison to chemical pollutants.

3. Results

3.1. Bacterial inactivation kinetic

In order to evaluate the evolution of bacterial inactivation, results from experimental set A were analyzed. In this set of experiments, the disinfection treatment was applied using ultrapure water solution and bacteria concentration was determined at time intervals between 0 and 120 min. Light intensity and TiO_2 concentration were constant and equal to 500 W/m^2 and 1 g/l, respectively.

Fig. 1 shows the results of *E.coli*, and *Enterococcus sp.* inactivation after the treatment and the fitting of the four previously mentioned models to the experimental data. The graphics are on logarithmic scale. As could be seen, inactivation rate of both bacteria is more slowly at the end of the treatment, possibly because of the adaptation of microorganisms to environmental conditions, prevalence of resistant bacteria or because products from bacterial lysis could compete with residual bacteria for the reaction with hydroxyl radicals [10,45]. Aiming to complement the results showed in Fig. 1, Table 3 compiles the value of the parameters of the models and the value of SRRC, the objective function that was minimized and with which it is possible to assess the quality of the fitting. Among the selected mathematical models, Gompertz model describe properly bacterial inactivation by means of TiO_2 photocatalysis.

According to the literature, [7,46–48]. *E. coli* inactivation is quicker than *Enterococcus sp.* inactivation in an ultrapure saline solution. The difference in the inactivation rate correlates with the structural differences between Gram-negative bacteria (*E. coli*) and Gram-positive (*Enterococcus sp.*). *Enterococcus sp.* showed more resistance to the photocatalytic treatment. Usual explanations for this difference in behavior are based on the differences between Gram-positive and Gram-negative cell wall. The peptidoglycan is the layer responsible for the rigidity in bacteria and in Gram-positive bacteria, it represents up to 90% of the cell wall, while in Gram-negative it only constitutes a 10% [46]. Moreover, in Gram-negative bacteria, there is an external membrane above the peptidoglycan layer, and one of the main components is the lipopolysaccharide, which is susceptible to oxidative attack and whose destruction is responsible for the inactivation of a lot of Gram-negative bacteria [49]. The values of residual activity (a_R), were close to zero, indicating that most of the bacteria in the water solution are removed after the treatment.

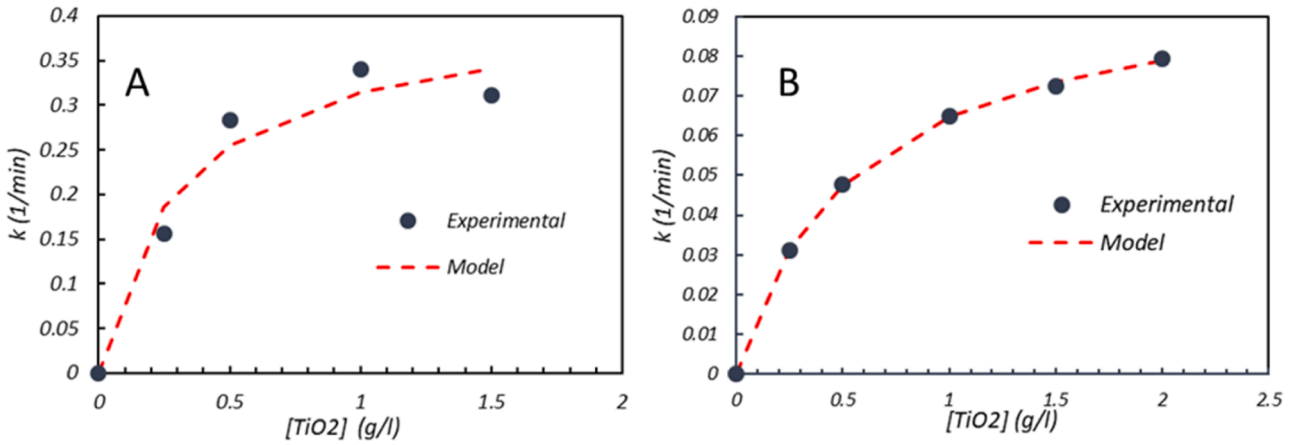

Fig. 2.. Dependence of the inactivation constant on TiO_2 concentration of *E. coli* (A) and *Enterococcus sp.* (B).

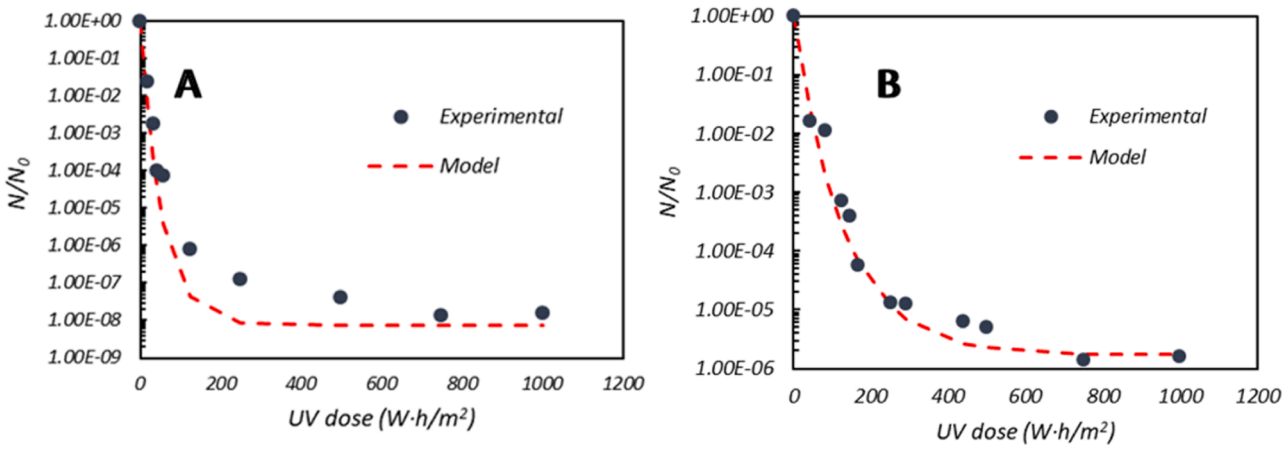

Fig. 3.. Evolution of bacterial concentration with UV-A dose for *E. coli* (A) and *Enterococcus sp*. (B).

Table 4
Kinetic and statistical results for applying Gompertz model to experimental set D.

Parameters	*E. coli*	*Enterococcus sp.*
k_{max} (m^2/ *W* •min)	$4.072•10^{-4}$	$2.000•10^{-4}$
a_R	$7.27•10^{-9}$	$1.69•10^{-6}$
RRMSE	5.900	2.928

3.2. *Operational conditions influence*

One of the main aims of this work was to obtain an expression for a kinetic model in which include the dependence of as many operational variables as possible, so that this kinetic model could be easily used for engineering purposes. As the Gompertz model has been chosen, the influence of the operational variables could be included in its kinetic constant.

In experimental set C (see Table 2), the influence of catalyst concentration was assessed by experimentally calculating bacterial concentration at 10 min of treatment for several TiO_2 concentrations in the range 0–2 g/l. The values of inactivation constants (k_I) at different TiO_2 concentrations were calculated assuming Gompertz model and setting the value of residual activity (a_R) obtained from experimental set A. All the experiments were carried out in ultrapure saline solution and applying 500 W/m^2 of light intensity, as in experimental set A. Fig. 2 shows that, for both bacteria, the value of the kinetic constant increases with the catalyst concentration until reaching a saturation value above which, the inactivation constant does not increase more. Some researchers report that, in photocatalytic processes in general, reaction rate increases with catalyst concentration, until reaching a saturation value [50–52]. This behavior could be attributed to the fact that TiO_2 particles have a diameter of 20–30 nm, while bacteria have an average diameter of 1 μm, therefore TiO_2 particles have to adsorb to bacterial surface. If catalyst concentration is high, all bacterial surface will be covered by catalyst particles. Moreover, as a consequence of increasing TiO_2 concentration, catalyst particles start to form aggregates up to 500 nm, thus the catalytic surface significantly decreases [50–52]. Finally, absorption and scattering effects due to TiO_2 particles have to be taken into account, since at high TiO_2 concentrations, the UV light intensity that reaches distant areas from the lamp will decrease.

Fig. 3 shows the results of the effect of light intensity. The inactivation constant increases linearly with light intensity, as other authors suggested [53,54]. It also increases with TiO_2 concentration until reaching a saturation value. This information can be complemented with the kinetic and statistical results obtained for both bacteria, which are collected in Table 4. As it can be seen the value of residual activity (a_R) for Enterococcus sp. are quite similar to the obtained in the experimental set A (a_R =$1.83·10^{-6}$). However, the a_R calculated for set A was a_R = $9.5·10^{-8}$). As a result, it can be concluded that experimental data fit better for *Enterococcus sp*. than for *E. coli*. This better validation of the model for *Enterococcus sp*. could be in some way expected, since the Gompertz model was not the one that best fitted inactivation data in experimental set A for *E. coli*. However, among studied models, Gompertz model is the only one that fits both bacteria in an acceptable range."

Table 5
Inactivation Gompertz kinetic constants in real WWTP.

Parameter	*E. coli*	*Enterococcus sp.*
a_R	$8.94.10^{-8}$	$8.95.10^{-8}$
$k_i 10^{-3}$ (min^{-1})	4.34 ± 1.07	4.52 ± 2.58

Finally, for study the influence of the matrix, in experimental set B (see Table 2), four WWTP water samples were analyzed, and after applying the disinfection treatment, bacterial concentration at 120 min were determined. Light intensity and TiO_2 concentration were the same as in experimental set A. For the four water samples and for *E. coli* and *Enterococcus sp.* the value of inactivation constant (k_I) was calculated by fitting the experimental values to the corresponding equation by non linear regression. These values of kinetic constants are shown in Table 5, as well as the inactivation constant in ultrapure saline solution (obtained from experimental set A).

As it could be expected, k_I is greater in saline solution (see Table 3) than in WWTP water sample, what proves that the presence of other inorganic or organic molecules slows down bacterial inactivation, since these molecules could compete with bacteria for the reaction with hydroxyl radicals. This effect could be reflected in the Gompertz constant by means of the effectiveness factor (η_G). This factor multiplies the inactivation constant in ultrapure water and was calculated by dividing the average value of k_I, in wastewater between the value of k_I in an ultrapure solution. In brief, including the effect of each studied operational conditions, the equation obtained for the inactivation constant of Gompertz model was purposed in order to model this behavior by:

$$k_I = \eta_G \cdot \frac{k_{max} \cdot I \cdot [TiO_2]}{K_{TiO_2} + [TiO_2]} \quad (4)$$

Where k_{max} and K_{TiO2} are kinetic parameters experimentally determined for each bacteria and $\eta_G$could be defined as an effectiveness factor to correct the value of the kinetic constant when the disinfection treatment is applied in water samples from WWTP instead of in an ultrapure saline solution. K_{TiO2} could be considered as a parameter that quantifies the affinity between the catalyst and the bacteria, in a way that the greater this parameter is, the less affinity for the catalyst the bacteria

has. *I* parameter is the radiation applied in a concrete period of time.

3.3. Photo-reactor design and optimization

As it was mentioned in section 2.6, the basic assumptions for an annular reactor are: (i) laminar regime, (ii) negligible radial and longitudinal diffusional effects, (iii) steady state, and (iv) isothermal operation. In addition, it is assumed that the concentration of TiO_2 keeps constant along the whole volume of the reactor. The assumption of laminar regime operation, which implies low rate of the axial velocity, is based on the fact that the rates of disinfection are usually slow, in comparison with the kinetics of organic contaminant removal, where it is possible to operate in turbulent regime and therefore with high circulation rates [10,44].

Laminar regime operation implies a radial dependence of bacteria concentration, and, in this case, of the radiation intensity, since the process implies a photocatalytic reaction. However, diffusional effects in axial and radial directions have been neglected due to the high weight of the bacteria, compared to that of a chemical molecule. In any case, the operation in laminar regime is conditioned by the parabolic radial profile of the velocity. Therefore, the design equation for the photo-reactor will be obtained from the mass balance for bacteria in a differential element of the annular laminar reactor.

Assuming the Gompertz model for the kinetics of bacterial inactivation, the equation of reactor design can be expressed as follows:

$$v_z(r)\cdot\frac{dN(r)}{dz}+k_I(r)\cdot N(r)\cdot\ln\left(\frac{N(r)}{N_R}\right)=0 \tag{5}$$

Where z and r are the axial and radial coordinates, $N(r)$ is the bacterial concentration at a given radial position (r), N_R is the residual bacterial concentration and $v_z(r)$ is the axial fluid velocity at r. For a steady laminar flow of a Newtonian fluid in an annular reactor, the radial profile of velocities for a given flowrate of liquid feed to the reactor, Q_0, is given by the following expression [55]:

$$v(r)=\frac{2\cdot Q_0}{\pi\cdot\left(R_1^2+R_2^2\right)}\cdot\frac{\ln\left(\frac{r}{R_1}\right)-\left(\frac{r^2-R_1^2}{R_2^2-R_1^2}\right)\cdot\ln\left(\frac{R_2}{R_1}\right)}{\ln\left(\frac{R_2}{R_1}\right)-\frac{\left(R_2^2-R_1^2\right)}{\left(R_2^2+R_1^2\right)}}\quad;\quad R_1<r\le R_2 \tag{6}$$

In addition, the pressure drop of the fluid for a given value of Q_0 is:

$$\left(-\frac{dp}{dz}\right)=\frac{8\cdot\mu\cdot Q_0}{\pi}\cdot\frac{\ln(R_2/R_1)}{\left(R_2^4-R_1^4\right)\cdot\ln(R_2/R_1)+\left(R_2^2-R_1^2\right)^2} \tag{7}$$

In the above equations R_1 and R_2 are the internal and external radius of the annular reactor and μ is the viscosity of the fluid. From Eq. (7), it can be deduced that the pressure drop strongly increases as the value of R_2 approaches that of R_1.

On the other side, assuming a linear dependence of the apparent extinction coefficient, ε_{app}, with the TiO_2 concentration, Lambert-Beer's law for the radial variation of light intensity can be expressed as:

$$I(r)=I_0\cdot\exp\left(-\varepsilon_{app}\cdot\left(r-R_1\right)\right)=I_0\cdot\exp\left(-\left(\varepsilon_0+\varepsilon\cdot[TiO_2]\right)\cdot\left(r-R_1\right)\right) \tag{8}$$

Where: I_0 is the lamp light intensity and ε_0 is the intrinsic extinction coefficient of pure water that it is assumed negiblible against the effect of the presence of dispersed TiO_2 in the solution, ε is the characteristic parameter related to the effective extinction coefficient due to the presence of TiO_2. Combining Eqs. (4), (6), and (8), the term k_{eff} can be defined as the "effective inactivation constant". This term has dimension of length^{-1}, and it is a function of r and catalyst concentration:

$$k_{eff}(r)=\frac{k_I(r)}{v(r)}=\frac{\eta_G\cdot k_{max}\cdot I_0\cdot[TiO_2]}{K_{TiO_2}+[TiO_2]}\cdot\frac{\exp\left(-\varepsilon\cdot[TiO_2]\cdot(r-R_1)\right)}{v(r)} \tag{9}$$

As the amount of catalyst increases, the inactivation rate also increases and the necessary length to reach a certain cellular conversion decreases. However, from Eq. (9) it is follow that, for each value of r, the "effective inactivation constant" goes through a maximum as a function of the catalyst concentration, named as $[TiO_2]_{opt}(r)$. This value can be calculated from the following condition:

$$\frac{dk_{eff}(r)}{d[TiO_2]}=0\quad\rightarrow\quad[TiO_2]_{opt}(r)=\frac{K_{TiO_2}}{2}\cdot\left(\sqrt{1+\frac{4}{K_{TiO_2}\cdot\varepsilon\cdot(r-R_1)}}-1\right) \tag{10}$$

In addition to the mathematical explanation, some physical phenomena can explain the existence of an optimum value. In the first place, high TiO_2 concentrations implies that bacterial surface will be covered by catalyst particles and no more could join the surface. Simultaneously, the particles could begin to form aggregates up to 500 nm, and consequently, the catalytic surface decreases [50–52]. Interestingly, the existence of a maximum value for the effective inactivation constant, implies that for a given degree of microbial inactivation, X_{cell}, the volume of the reactor will be minimum, and the optimization of the reactor is attained through the optimization of TiO_2 concentration.

Solving Eq. (5), taking $N=N_0$ at $z=0$, it is obtained the value of the bacteria concentration at the exit of each radial position of the reactor:

$$N(r)=N_0\cdot\left(\frac{N_R}{N_0}\right)^{1-\exp\left(-k_{eff}(r)\cdot z\right)}=N_0\cdot(a_R)^{1-\exp\left(-k_{eff}(r)\cdot z\right)} \tag{11}$$

In the above solution it has been considered the laminar reactor as an infinite sequence of individual plug-flow reactors concentrically placed between R_1 and R_2. Consequently, the total mass flowrate of cells at the exit of the photo-reactor is given by:

$$F_{cell,exit}=\int_{R_1}^{R_2}N(r)\cdot dQ=2\pi\cdot N_0\cdot\int_{R_1}^{R_2}(a_R)^{1-\exp\left(-k_{eff}(r)\cdot z\right)}\cdot v(r)\cdot dr \tag{12}$$

Finally, the cellular conversion is given by the following expression:

$$X_{cell}=1-\frac{F_{cell,exit}}{F_{cell,inlet}}=1-\frac{\int_{R_1}^{R_2}N(r)\cdot dQ}{N_0\cdot Q_0}=1-\frac{2\pi}{Q_0}\cdot\int_{R_1}^{R_2}(a_R)^{1-\exp\left(-k_{eff}(r)\cdot z\right)}\cdot v(r)\cdot r\cdot dr \tag{13}$$

For a given length of the reactor, z, the conversion will be maximum if the catalyst concentration is the optimum. This global value can be obtained from the following condition:

$$\frac{dX_{cell}}{d[TiO_2]}=0\quad\rightarrow\quad\begin{cases}X_{cell},\ \max\\ [TiO_2]_{opt}\end{cases} \tag{14}$$

The above condition must be solved numerically, and the value $[TiO_2]_{opt}$ obtained is an averaged value of that obtained from Eq. (10) in combination with Eq. (13). After calculation of the $[TiO_2]_{opt}$, Eq. (13) can be solved by radial discretization and numerical integration. This Eq. (13) can be used, to estimate the size of the photo-rector, i.e. length (z), and R_2, for a specified value R_1, necessary to attain a given cellular conversion, processing a flowrate Q_0. Alternatively, also can be used to calculate the cell conversion at the exit of the reactor and the amount of TiO_2, knowing the values of z and R_2. Finally, the power lamp light intensity (I_0), assuming that the lamp has the same length as the reactor, can be estimated as:

$$W=2\pi\cdot R_1\cdot I_0\cdot z \tag{15}$$

In any case, all the solutions reached in the calculation of the reactor, must fulfill the following restrictions:

i) The regime of circulation of the fluid must be laminar, therefore:

$$\mathrm{Re}=\frac{\langle v\rangle\cdot D_{eq}\cdot\rho_f}{\mu_f}=\frac{2\left(R_2-R_1\right)\cdot\langle v\rangle\cdot\rho_f}{\mu_f}=\frac{2\cdot Q_0\cdot\rho_f}{\pi\cdot\mu_f\cdot\left(R_2+R_1\right)}\le 2100 \tag{16}$$

Therefore, for the case of water stream, $\rho\cong$ 1000 kg/m^3; $\mu\cong$ 0.001 (kg/m.s), the minimum value for R_2 will be given by:

Table 6
Design of laminar annular photo-reactor. Influence of external radius.

R_2 (m)	0.102	0.100	0.090	0.080	0.070	0.060	0.050	0.040
Re	1114	1134	1228	1340	1474	1637	1842	2100
Average rate (m/s)	0.0077	0.0081	0.0102	0.0134	0.0184	0.0273	0.0461	0.1032
Ratio: Aver. liquid rate / Sedim. Rate	5000	5258	6645	8699	11,962	17,721	29,904	67,015
[TiO_2] optim. (g/l)	0.234	0.240	0.271	0.311	0.367	0.452	0.598	0.932
Reactor lenght (m)	1.604	1.649	1.875	2.177	2.606	3.271	4.477	7.523
Reactor volume (l)	48.2	47.1	42.4	37.6	32.8	27.7	22.5	16.9
Average residence time (min)	3.5	3.4	3.1	2.7	2.4	2.0	1.6	1.2
Mass of TiO_2 (g)	11.27	11.31	11.48	11.69	12.01	12.53	13.46	15.73
Pressure drop (bar)	0.28	0.32	0.63	1.38	3.56	11.81	61.59	898.75

$$R_2 \geq \frac{2\cdot Q_0\cdot \rho_f}{2100\cdot \pi\cdot \mu_f} - R_1 \cong 303.15\cdot Q_0 - R_1 \tag{17}$$

ii) In order to avoid any significant sedimentation of the cells and/or the catalysts particles, it is assumed that the average rate of the fluid must be 5000 times the higher of the two sedimentation rates:

$$\frac{\langle v\rangle_f}{v_{sed}} = \frac{Q_0}{\pi\cdot\left(R_2^2 - R_1^2\right)\cdot v_{sed}} \geq 5000 \tag{18}$$

The rate of sedimentation can be estimated using the following formula:

$$v_{sed} = \frac{d_p^2\cdot\left(\rho_p - \rho_f\right)\cdot g}{18\cdot\mu_f} \tag{19}$$

Where: d_p is the average particle diameter, and ρ_p the density of the particle. For the TiO_2 particles, ρ_p= 4200 kg/m^3, of 20–30 nm, which can form aggregates up to 500 nm, the rate of sedimentation is around $v_{sed,TiO_2} = 4.43\cdot10^{-7}$m/s [18]. Estimations of sedimentation rate of bacteria in water give a value of $v_{sed,cell} = 1.54\cdot10^{-6}$ m/s [56]. Taking the value of the v_{sed} of bacteria, the rate of fluid must be:$\langle v\rangle_f \geq 0.0077$ m/s. Therefore, for a given value of R_1, the upper limit of R_2 can be estimated as:

$$R_2 \leq \sqrt{R_1^2 + \frac{Q_0}{\pi\cdot v_{sed}}} \cong \sqrt{R_1^2 + 41.34\cdot Q_0} \tag{20}$$

Therefore, Eqs. (17) and (20) define the interval of valid values for R_2, for a set of values of R_1 and Q_0. In addition, in all the cases, the pressure drop of the fluid in the reactor must be lowest possible, therefore, according to Eq. (7), the value of R_2 should be the higher possible, which is given by Eq. (20).

The other important factor in the operation of the reactor is the amount of TiO_2 needed to reach the desired cell conversion at the exit of the photo-reactor. From the value of $[TiO_2]_{opt}$, the amount of TiO_2 is calculated as:

$$mass_{TiO_2} = z\cdot\pi\cdot\left(R_2^2 - R_1^2\right)\cdot[TiO_2]_{opt} \tag{21}$$

As illustrative example of application of the model developed in this study, Table 6 shows the design of the laminar photo-reactor for *Enterococcus sp.* Inactivation. Thus, Table 6 summarizes the results of the influence of the external radius (R_2) in the design parameters within the limit values defined in Eqs. (17) and (20). These calculations are made for the following data of design: Q_0 = 20 m^3/h, X_{cell} = 0.999, R_1 = 0.03 m (extracted from previous photocatalytic bench-reactor design in the literature conducted by Marugán et al. [44]), effectiveness factor, η_G = 0.2, k_{max}= 2·10^{-4} m^2·L/(g·W·h), K_{TiO2}= 0.558 g/L, I_0= 750 W/m^2, ε_{app}= 72 m^{-1}. For the application of the model, the following algorithm has been used: (i) calculation of the minimum and maximum values of R_2 satisfying the conditions given in Eqs. (17) and (20); (ii) for each selected value of R_2, and for an initial guess of the value of the reactor length, z, estimation of $[TiO_2]_{opt}$ using Eq. (14); (iii) If the value of X_{cell} is lower than the design value, 0.999 in this case, re-calculation of z using Eq. (13), until the desired conversion is achieved. This algorithm has been implemented in Excel®, using SOLVER® complement for steps (ii) and (iii). The numerical solution of Eq. (13) has been done by means of Simpsons' rule, using 5000 steps of radial increment, i.e. $\Delta r = (R_2\text{-}R_1)/5000$.

From the values show in Table 6, it is clear that the most favorable case corresponds to the higher value of R_2 (R_2 = 0.1023 m). In this case, although the volume of the reactor is the higher, the pressure drop and amount of TiO_2 are the lowest. Therefore, given that the conditions of no-sedimentation and laminar flow are fulfilled, this value will be selected as the design value. Other authors have been previously pointed that photoreactors should work below the saturation level of TiO_2 to ensure an efficient absorption and to save catalyst costs [10].

4. Conclusions

In this study, promising results have been achieved in the design of heterogeneous photocatalytic reactors. Initially, experimental data were collected at laboratory scale for the inactivation of *E. Coli* and *Enterococcus sp.*, and a Gompertz kinetic model was proposed to model photocatalytic inactivation of both bacteria. As a result, the kinetic constant of the Gompertz model was defined, incorporating the influence of key operational variables on the photocatalytic inactivation of pathogenic coliforms, such as radiation intensity, catalyst concentration, and matrix influence.

Furthermore, an analytical model was developed to design and optimize a pilot-scale laminar photocatalytic annular reactor, based on the intrinsic kinetics and its geometry. This model has been applied to a real WWTP effluent operating under laminar regime. In this context, it was assumed that radiation intensity follows the Lambert-Beer law, and mathematical analysis was conducted to evaluate the impact of the external reactor radius on the other design parameters. Based on the kinetic parameters determined at laboratory scale, the design parameters that optimize reactor operation by minimizing both pressure drop and catalyst concentration have been determined. The algorithm of resolution and optimization of the laminar reactor model proposed here can be directly applied to include other kinetic models of bacterial inactivation. "This analytical model provides a useful tool for reactor optimization, although authors acknowledge that it may not address all the aspects presented by a real plant. Therefore, authors emphasize the importance of validating this theoretical model to ensure its feasibility and effectiveness for large-scale photoreactor systems.

CRediT authorship contribution statement

Moreno Raúl: Data curation, Formal analysis. **Mosteo Rosa:** Conceptualization, Funding acquisition, Investigation, Methodology, Writing – review & editing. **Monzón Antonio:** Conceptualization, Investigation, Resources, Software, Supervision, Writing – review & editing. **Moles Samuel:** Conceptualization, Formal analysis, Investigation, Writing – original draft, Writing – review & editing. **Ormad Maria P.:** Investigation, Methodology, Project administration, Supervision.

Declaration of Competing Interest

The authors declare that they have no known competing financial interests or personal relationships that could have appeared to influence the work reported in this paper.

Data availability

Data will be made available on request.

Acknowledgments

This special issue is dedicated to honor the retirement of Prof. Santiago Esplugas at the University of Barcelona (UB, Spain), a key figure in the area of Catalytic Advanced Oxidation Processes. This work was funded by the grant TED2021-129267B-I00 funded by MCIN/AEI/10.13039/501100011033 and by the "European Union NextGenerationEU/PRTR. Samuel Moles thanks the grant Margarita Salas funded by the European Union-NextGenerationEU. Authors thank also the Regional Government of Aragón under the Research Groups Support Program (B43_23R: Agua y Salud Ambiental and T22_23R: Grupo de Procesos Termoquímicos).

References

[1] A. Chokshi, Z. Sifri, D. Cennimo, H. Horng, Global contributors to antibiotic resistance, J. Glob. Infect. Dis. 11 (2019) 36–42, https://doi.org/10.4103/jgid.jgid_110_18.

[2] R. Laxminarayan, A. Duse, C. Wattal, A.K.M. Zaidi, H.F.L. Wertheim, N. Sumpradit, E. Vlieghe, G.L. Hara, I.M. Gould, H. Goossens, C. Greko, A.D. So, M. Bigdeli, G. Tomson, W. Woodhouse, E. Ombaka, A.Q. Peralta, F.N. Qamar, F. Mir, S. Kariuki, Z.A. Bhutta, A. Coates, R. Bergstrom, G.D. Wright, E.D. Brown, O. Cars, Antibiotic resistance-the need for global solutions, Lancet Infect. Dis. 13 (2013) 1057–1098, https://doi.org/10.1016/S1473-3099(13)70318-9.

[3] WHO, Emerging Issues in Water and Infectious Disease, 2003, p. 24.

[4] O.S. Samuel, E.C. PraiseGod, T.I. Theophilus, K.C. Omolola, Human health risk assessment data of trace elements concentration in tap water—Abeokuta South, Nigeria, Data Br. 18 (2018) 1416–1426, https://doi.org/10.1016/j.dib.2018.04.041.

[5] L. De Jong, A. Kemp, Stoicheiometry and kinetics of the prolyl 4-hydroxylase partial reaction, Biochim. Biophys. Acta Protein Struct. Mol. 787 (1984) 105–111, https://doi.org/10.1016/0167-4838(84)90113-4.

[6] J. Rodríguez-Chueca, M. Morales, R. Mosteo, M.P. Ormad, J.L. Ovelleiro, Inactivation of Enterococcus faecalis, Pseudomonas aeruginosa and Escherichia coli present in treated urban wastewater by coagulation-flocculation and photo-Fenton processes, Photochem. Photobiol. Sci. 12 (2013) 864–871, https://doi.org/10.1039/c3pp25352j.

[7] P. Valero, R. Mosteo, M.P. Ormad, L. Lázaro, J.L. Ovelleiro, Inactivation of Enterococcus sp. by conventional and advanced oxidation processes in synthetic treated urban wastewater, Ozone Sci. Eng. 37 (2015) 467–475, https://doi.org/10.1080/01919512.2015.1042572.

[8] M. Lanao, M.P. Ormad, R. Mosteo, J.L. Ovelleiro, Inactivation of Enterococcus sp. by photolysis and TiO 2 photocatalysis with H2O2 in natural water, Sol. Energy 86 (2012) 619–625, https://doi.org/10.1016/j.solener.2011.11.007.

[9] K. Siddique, Different heavy metal concentrations in plants and soil irrigated with industrial / sewage waste water, Int. J. Environ. Monit. Anal. 2 (2014) 151, https://doi.org/10.11648/j.ijema.20140203.14.

[10] M.N. Chong, B. Jin, C.W.K. Chow, C. Saint, Recent developments in photocatalytic water treatment technology: a review, Water Res 44 (2010) 2997–3027, https://doi.org/10.1016/j.watres.2010.02.039.

[11] S. Chowdhury, J. Sikder, T. Mandal, G. Halder, Comprehensive analysis on sorptive uptake of enrofloxacin by activated carbon derived from industrial paper sludge, Sci. Total Environ. 665 (2019) 438–452, https://doi.org/10.1016/j.scitotenv.2019.02.081.

[12] D.B. Miklos, C. Remy, M. Jekel, K.G. Linden, J.E. Drewes, U. Hübner, Evaluation of advanced oxidation processes for water and wastewater treatment – A critical review, Water Res 139 (2018) 118–131, https://doi.org/10.1016/j.watres.2018.03.042.

[13] S. Lim, J.L. Shi, U. von Gunten, D.L. McCurry, Ozonation of organic compounds in water and wastewater: a critical review, Water Res 213 (2022) 118053, https://doi.org/10.1016/j.watres.2022.118053.

[14] F.A. Almomani, R.R. Bhosale, M.A.M.M. Khraisheh, A. Kumar, C. Kennes, Mineralization of dichloromethane using solar-oxidation and activated TiO2: pilot scale study, Sol. Energy 172 (2018), https://doi.org/10.1016/j.solener.2018.07.042.

[15] A.K. Behera, K.P. Shadangi, P.K. Sarangi, Synthesis of dye-sensitized TiO2/Ag doped nano-composites using UV photoreduction process for phenol degradation: a comparative study, Environ. Pollut. 312 (2022) 120019, https://doi.org/10.1016/j.envpol.2022.120019.

[16] A. Kutuzova, T. Dontsova, W. Kwapinski, Application of tio2-based photocatalysts to antibiotics degradation: cases of sulfamethoxazole, trimethoprim and ciprofloxacin, Catalysts 11 (2021), https://doi.org/10.3390/catal11060728.

[17] Y. Deng, R. Zhao, Advanced oxidation processes (AOPs) in wastewater treatment, Curr. Pollut. Rep. 1 (2015) 167–176, https://doi.org/10.1007/s40726-015-0015-z.

[18] O.K. Dalrymple, E. Stefanakos, M.A. Trotz, D.Y. Goswami, A review of the mechanisms and modeling of photocatalytic disinfection, Appl. Catal. B Environ. 98 (2010) 27–38, https://doi.org/10.1016/j.apcatb.2010.05.001.

[19] A. Pal, S.O. Pehkonen, L.E. Yu, M.B. Ray, Photocatalytic inactivation of gram-positive and gram-negative bacteria using fluorescent light, J. Photochem. Photobiol. A Chem. 186 (2007) 335–341, https://doi.org/10.1016/j.jphotochem.2006.09.002.

[20] K.P. Kühn, I.F. Chaberny, K. Massholder, M. Stickler, V.W. Benz, H.G. Sonntag, L. Erdinger, Disinfection of surfaces by photocatalytic oxidation with titanium dioxide and UVA light, Chemosphere 53 (2003) 71–77, https://doi.org/10.1016/S0045-6535(03)00362-X.

[21] M. Conde-Cid, C. Álvarez-Esmorís, R. Paradelo-Núñez, J.C. Nóvoa-Muñoz, M. Arias-Estévez, E. Álvarez-Rodríguez, M.J. Fernández-Sanjurjo, A. Núñez-Delgado, Occurrence of tetracyclines and sulfonamides in manures, agricultural soils and crops from different areas in Galicia (NW Spain), J. Clean. Prod. 197 (2018) 491–500, https://doi.org/10.1016/j.jclepro.2018.06.217.

[22] C.M. Núñez-Núñez, G.I. Osorio-Revilla, I. Villanueva-Fierro, C. Antileo, J.B. Proal-Nájera, Solar fecal coliform disinfection in awastewater treatment plant by oxidation processes: Kinetic analysis as a function of solar radiation, Water 12 (2020) 1–16, https://doi.org/10.3390/w12030639.

[23] H. Chick, An investigation of the laws of disinfection, J. Hyg. 8 (1908) 92–158, https://doi.org/10.1017/S0022172400006987.

[24] C. Sordo, R. Van Grieken, J. Marugán, P. Fernández-Ibáñez, Solar photocatalytic disinfection with immobilised TiO2 at pilot-plant scale, Water Sci. Technol. 61 (2010), https://doi.org/10.2166/wst.2010.876.

[25] C. Casado, R. Timmers, A. Sergejevs, C.T. Clarke, D.W.E. Allsopp, C.R. Bowen, R. van Grieken, J. Marugán, Design and validation of a LED-based high intensity photocatalytic reactor for quantifying activity measurements, Chem. Eng. J. 327 (2017) 1043–1055, https://doi.org/10.1016/j.cej.2017.06.167.

[26] R. van Grieken, J. Marugán, C. Pablos, L. Furones, A. López, Comparison between the photocatalytic inactivation of gram-positive E. faecalis and Gram-negative E. coli faecal contamination indicator microorganisms, Appl. Catal. B Environ. 100 (2010) 212–220, https://doi.org/10.1016/j.apcatb.2010.07.034.

[27] J. Marugán, R. Van Grieken, C. Pablos, M.L. Satuf, A.E. Cassano, O.M. Alfano, Kinetic modelling of Escherichia coli inactivation in a photocatalytic wall reactor, Catal. Today 240 (2015) 9–15, https://doi.org/10.1016/j.cattod.2014.03.005.

[28] J. Marugán, R. van Grieken, C. Pablos, M.L. Satuf, A.E. Cassano, O.M. Alfano, Rigorous kinetic modelling with explicit radiation absorption effects of the photocatalytic inactivation of bacteria in water using suspended titanium dioxide, Appl. Catal. B Environ. 102 (2011) 404–416, https://doi.org/10.1016/j.apcatb.2010.12.012.

[29] S. Moles, R. Mosteo, J. Gómez, J. Szpunar, S. Gozzo, J.R. Castillo, M.P. Ormad, Towards the removal of antibiotics detected in wastewaters in the POCTEFA territory: occurrence and TiO2 photocatalytic pilot-scale plant performance, Water 12 (2020) 1–26, https://doi.org/10.3390/w12051453.

[30] S.K. Loeb, P.J.J. Alvarez, J.A. Brame, E.L. Cates, W. Choi, J. Crittenden, D. D. Dionysiou, Q. Li, G. Li-Puma, X. Quan, D.L. Sedlak, T. David Waite, P. Westerhoff, J.H. Kim, The technology horizon for photocatalytic water treatment: sunrise or sunset? Environ. Sci. Technol. 53 (2019) 2937–2947, https://doi.org/10.1021/acs.est.8b05041.

[31] J. Chen, S. Loeb, J.H. Kim, LED revolution: fundamentals and prospects for UV disinfection applications, Environ. Sci. Water Res. Technol. 3 (2017) 188–202, https://doi.org/10.1039/c6ew00241b.

[32] A.E. Cassano, O.M. Alfano, Reaction engineering of suspended solid heterogeneous photocatalytic reactors, Catal. Today 58 (2000) 167–197, https://doi.org/10.1016/S0920-5861(00)00251-0.

[33] A.E. Cassano, C.A. Martín, R.J. Brandi, O.M. Alfano, Photoreactor analysis and design: fundamentals and applications, Ind. Eng. Chem. Res. 34 (1995) 2155–2201, https://doi.org/10.1021/ie00046a001.

[34] G. Li Puma, V. Puddu, H.K. Tsang, A. Gora, B. Toepfer, Photocatalytic oxidation of multicomponent mixtures of estrogens (estrone (E1), 17β-estradiol (E2), 17α-ethynylestradiol (EE2) and estriol (E3)) under UVA and UVC radiation: photon absorption, quantum yields and rate constants independent of photon absorp, Appl. Catal. B Environ. 99 (2010) 388–397, https://doi.org/10.1016/j.apcatb.2010.05.015.

[35] O. Autin, J. Hart, P. Jarvis, J. MacAdam, S.A. Parsons, B. Jefferson, Comparison of UV/TiO2 and UV/H2O2 processes in an annular photoreactor for removal of micropollutants: influence of water parameters on metaldehyde removal, quantum yields and energy consumption, Appl. Catal. B Environ. 138–139 (2013) 268–275, https://doi.org/10.1016/j.apcatb.2013.02.045.

[36] E.R. De Bernardez, A.E. Cassano, A priori design of a continuous annular photochemical reactor: experimental validation for simple reactions, J. Photochem. 30 (1985) 285–301, https://doi.org/10.1016/0047-2670(85)85049-8.

[37] S. Malato, P. Fernández-Ibáñez, M.I. Maldonado, J. Blanco, W. Gernjak, Decontamination and disinfection of water by solar photocatalysis: recent overview and trends, Catal. Today 147 (2009) 1–59, https://doi.org/10.1016/j.cattod.2009.06.018.

[38] D.F. Ollis, E. Pelizzetti, N. Serpone, Destruction of water contaminants, Environ. Sci. Technol. 25 (1991) 1522–1529, https://doi.org/10.1021/es00021a001.
[39] D.F. Ollis, N. Serpone, Gsot Features, 25 (1991).
[40] A. Visan, J.R. Van Ommen, M.T. Kreutzer, R.G.H. Lammertink, Photocatalytic reactor design: guidelines for kinetic investigation, Ind. Eng. Chem. Res. 58 (2019) 5349–5357, https://doi.org/10.1021/acs.iecr.9b00381.
[41] G. Li Puma, A. Brucato, Dimensionless analysis of slurry photocatalytic reactors using two-flux and six-flux radiation absorption-scattering models, Catal. Today 122 (2007) 78–90, https://doi.org/10.1016/j.cattod.2007.01.027.
[42] S. Moles, J. Berges, M.P. Ormad, M.J. Nieto-Monge, J. Gómez, R. Mosteo, Photoactivation and photoregeneration of TiO2/PAC mixture applied in suspension in water treatments: approach to a real application, Environ. Sci. Pollut. Res. (2021), https://doi.org/10.1007/s11356-021-12542-4.
[43] G.C. Roda, F. Santarelli, A rational approach to the design of photocatalytic reactors, Ind. Eng. Chem. Res. 46 (2007) 7637–7644, https://doi.org/10.1021/ie070302a.
[44] J. Marugán, R. van Grieken, C. Pablos, M.L. Satuf, A.E. Cassano, O.M. Alfano, Modeling of a bench-scale photocatalytic reactor for water disinfection from laboratory-scale kinetic data, Chem. Eng. J. 224 (2013) 39–45, https://doi.org/10.1016/j.cej.2012.11.082.
[45] P. Ganguly, A. Breen, S.C. Pillai, S. Panneri, U.S. Hareesh, Recent Advances in Photocatalytic Detoxification of Water, Elsevier Inc, 2019, https://doi.org/10.1016/B978-0-12-813926-4.00029-X.
[46] J. Rodríguez-Chueca, M.P. Ormad, R. Mosteo, J.L. Ovelleiro, Kinetic modeling of Escherichia coli and Enterococcus sp. inactivation in wastewater treatment by photo-Fenton and H2O2/UV–vis processes, Chem. Eng. Sci. 138 (2015) 730–740, https://doi.org/10.1016/j.ces.2015.08.051.
[47] S. Moles, P. Valero, S. Escuadra, R. Mosteo, J. Gómez, M.P. Ormad, Performance comparison of commercial TiO2: separation and reuse for bacterial photo-inactivation and emerging pollutants photo-degradation, Environ. Sci. Pollut. Res. (2020), https://doi.org/10.1007/s11356-019-07276-3.
[48] A. Erkan, U. Bakir, G. Karakas, Photocatalytic microbial inactivation over Pd doped SnO2 and TiO2 thin films, J. Photochem. Photobiol. A Chem. 184 (2006) 313–321, https://doi.org/10.1016/j.jphotochem.2006.05.001.
[49] J.F. Muir, M. Control, D. Resistance, Book Reviews, 123, 1994. 173–174.
[50] C.N. Haas, A mechanistic kinetic model for chlorine disinfection, Environ. Sci. Technol. 14 (1980) 339–340, https://doi.org/10.1021/es60163a012.
[51] A.I.C. J. Blanco Gálvez, S.Malato Rodríguez, J. Peral, B. Sánchez, Diseño de reactores para fotocatálisis: Evaluación comparativa de las distintas opciones. Part 2, 2015.available online: https://estrucplan.com.ar/diseno-de-reactores-para-fotocatalisis-evaluacion-comparativa-de-las-distintas-opciones-parte-2/.
[52] S. Malato, M.I. Maldonado, P. Fernández-Ibáñez, I. Oller, I. Polo, R. Sánchez-Moreno, Decontamination and disinfection of water by solar photocatalysis: the pilot plants of the plataforma solar de Almeria, Mater. Sci. Semicond. Process. 42 (2016) 15–23, https://doi.org/10.1016/j.mssp.2015.07.017.
[53] C. Wei, W.Y. Lin, Z. Zainal, N.E. Williams, K. Zhu, A.P. Kruzlc, R.L. Smith, K. Rajeshwar, Bactericidal activity of TiO2 photocatalyst in aqueous media: toward a solar-assisted water disinfection system, Environ. Sci. Technol. 28 (1994) 934–938, https://doi.org/10.1021/es00054a027.
[54] A.K. Benabbou, Z. Derriche, C. Felix, P. Lejeune, C. Guillard, Photocatalytic inactivation of Escherischia coli. Effect of concentration of TiO2 and microorganism, nature, and intensity of UV irradiation, Appl. Catal. B Environ. 76 (2007) 257–263, https://doi.org/10.1016/j.apcatb.2007.05.026.
[55] E.N.L.R. B. Bird, W.E. Stewart, Transport Phenomena, second Intern, 2002.
[56] Luis E. Pérez-Farrás, Cátedra hidráulica aplicada a la ingeniería sanitaria. [Buenos Aires]: Universidad de Buenos Aires; 2005.